A-769662 inhibits adipocyte glucose uptake in an AMPK-independent manner

Franziska Kopietz[1], Yazeed Alshuweishi[2,3], Silvia Bijland[2], Fatmah Alghamdi[2,4], Eva Degerman[1], Kei Sakamoto[5,6], Ian P. Salt[2] and Olga Göransson[1]

[1] Department of Experimental Medical Science, Lund University, Sweden

[2] Institute of Cardiovascular & Medical Sciences, College of Medical, Veterinary and Life Sciences, University of Glasgow, United Kingdom

[3] Department of Clinical Laboratory Sciences, King Saud University, Riyadh, Kingdom of Saudi Arabia

[4] Faculty of Medicine, King Abdulaziz University, Jeddah, Kingdom of Saudi Arabia

[5]Nestlé Research, EPFL Innovation Park, 1015, Lausanne, Switzerland

[6]Novo Nordisk Foundation Center for Basic Metabolic Research, University of Copenhagen, Copenhagen, Denmark

Corresponding author:

Franziska Kopietz

Lund University; Protein Phosphorylation Research Group

BMC C11, Klinikgatan 28; 22242 Lund SWEDEN

Telephone: +46 (0)46-2229552

E-mail: franziska.kopietz@med.lu.se

Abstract

Activation of AMP-activated protein kinase (AMPK) is considered a valid strategy for the treatment of type 2 diabetes. However, despite the importance of adipose tissue for whole-body energy homeostasis, the effect of AMPK activation in adipocytes has only been studied to a limited extent and mainly with the AMP-mimetic 5-aminoimidazole-4-carboxamide-1-β-d-ribofuranoside (AICAR), which has limited specificity. The aim of this study was to evaluate the effect of the allosteric AMPK activators A-769662 and 991 on glucose uptake in adipocytes. For this purpose, primary rat or human adipocytes, and cultured 3T3-L1 adipocytes, were treated with either of the allosteric activators, or AICAR, and basal and insulin-stimulated glucose uptake was assessed. Additionally, the effect of AMPK activators on insulin-stimulated phosphorylation of Akt and Akt substrate of 160 kDa was assessed. Furthermore, primary adipocytes from ADaM site binding drug-resistant AMPKβ1 S108A knock-in mice were employed to investigate specificity of the drugs for the observed effects. Our results show that insulin-stimulated adipocyte glucose uptake was significantly reduced by A-769662 but not 991, yet neither activator had any clear effects on basal or insulin-stimulated Akt/AS160 signaling. The use of AMPKβ1 S108A mutant-expressing adipocytes revealed that the observed inhibition of glucose uptake by A-769662 is most likely AMPK-independent, a finding which is supported by the rapid inhibitory effect A-769662 exerts on glucose uptake in 3T3-L1 adipocytes. These data suggest that AMPK activation *per se* does not inhibit glucose uptake in adipocytes and that the effects of AICAR and A-769662 are AMPK-independent.

Keywords

AMP-activated protein kinase, glucose uptake, insulin, adipocytes, A-769662, 991, S108A.

Introduction

AMP-activated protein kinase (AMPK) is a highly conserved heterotrimeric protein composed of a catalytic α-subunit and two regulatory subunits, β and γ. In the event of decreasing cellular energy levels, i.e. an increase in AMP and ADP, AMPK becomes activated. This activation involves the binding of AMP and/or ADP to the regulatory γ-subunit, and a subsequent net increase in phosphorylation of AMPKα on T172, by liver kinase B1 (LKB1) or Ca^{2+}/calmodulin-dependent protein kinase kinase-β (CaMKKβ) (1). Once activated, AMPK functions to shut off energy-consuming pathways and simultaneously to promote ATP-generating processes (2). Therefore, AMPK constitutes a key player in the regulation of cellular and whole-body energy homeostasis.

Activation of AMPK is considered a useful strategy for the treatment of type 2 diabetes (T2D), mainly due to beneficial effects observed in liver and muscle tissue, including decreased lipid accumulation and increased glucose uptake, respectively (2, 3). A commonly used AMPK activator is 5-aminoimidazole-4-carboxamide-1-β-D–ribofuranoside (AICAR), which is converted to AICAR monophosphate (ZMP) once it enters the cell, and acts as an AMP-mimetic (4-6). However, AICAR has limited specificity and several off-target effects have been reported (7-10). More specific AMPK activators including A-769662, a thienopyridone compound, and 991, a benzimidazone derivate have later been described (11, 12). Both of these compounds activate AMPK by binding to the allosteric drug and metabolite (ADaM) site, located at an interface between the α- and β-subunit. It has also been shown that ligand binding to the ADaM site requires, or is greatly increased by, phosphorylation of S108 in the β1-subunit (12, 13).

The effect of AMPK activators in liver and muscle has been extensively studied (14, 15). However, despite the role of adipose tissue in the development of insulin resistance – a key feature of T2D, the regulation of adipocyte metabolism by AMPK has been poorly characterized (16, 17). While we recently described the effect of AICAR and the ADaM site AMPK activators on lipolysis, adipocyte glucose uptake has only been studied using AICAR (18-20). To date, the results obtained with AICAR suggest increased basal and decreased insulin-stimulated glucose uptake in cultured 3T3-L1 adipocytes (20, 21). In isolated primary adipocytes, basal as well as insulin-stimulated glucose uptake was shown to be suppressed by AICAR. This was suggested to be due to reduced phosphorylation of the Akt substrate of 160 kDa (AS160) (19, 22). AS160 is a Rab-GAP (GTPase activating protein) that is inhibited upon Akt-mediated phosphorylation, thereby acting to link increased insulin signaling to trafficking/fusion of vesicles containing the insulin-sensitive glucose transporter type 4 (GLUT4) to the plasma membrane (23). Phosphorylation of AS160 in response to insulin also increases its association with the scaffold protein 14-3-3, an interaction important for GLUT4 trafficking in adipocytes (24, 25).

Although adipocytes account for a minor portion of total post-prandial glucose uptake, adipocyte-specific deletion of GLUT4 has been shown to induce insulin resistance in liver and muscle, leading to the development of glucose intolerance and hyperinsulinemia (16). These findings by Abel et al. highlight the importance of adipocyte glucose uptake as well as the necessity to further investigate the effect of AMPK activation on adipocyte glucose uptake with more selective drugs than AICAR.

The aim of the present study was to determine the effect of the ADaM site-binding AMPK activators A-769662 and 991, compared to that of AICAR, on glucose uptake in rodent and human adipocytes. This information is critical for a thorough

93 understanding of the effect of AMPK activators on adipose tissue metabolism and
94 thereby the suitability of AMPK activators as therapies for metabolic diseases,
95 including T2D.

Materials and Methods

Materials.

Insulin was purchased from Novo Nordisk (Copenhagen, Denmark). Complete protease-inhibitor cocktail was from Roche (Mannheim, Germany). Pre-cast Novex SDS Polyacrylamide Bis-Tris gels and DTT were purchased from Invitrogen (Carlsbad, USA). Dulbecco's Modified Eagle's Medium (DMEM), penicillin-streptomycin, 1,4-Bis(5-phenyl-2-oxazolyl)benzene, phenylisopropyl adenosine (PIA) and cytochalasin B were from Sigma Aldrich (St. Louis, MO, USA). ^{14}C-glucose and 2-[^{3}H]-deoxy-D-glucose were obtained from Perkin Elmer (Boston, USA). Enhanced chemiluminescent (ECL) substrates SuperSignal West Pico and SuperSignal West Femto were obtained from Thermo Fisher Scientific (Rockford, IL, USA). AICAR was purchased from Toronto Research Chemicals (Toronto, Canada) and 991 from AOBIOUS (Gloucester, MA, USA) for primary adipocytes or synthesized by MRC Technology (London, UK) for 3T3-L1 adipocytes. A-769662 was from Abcam (Cambridge, UK). Plasmids containing glutathione S-transferase (GST) or 14-3-3-GST were a generous gift from Prof. T. Palmer (Hull York Medical School, Hull, UK)

Antibodies.

The following primary antibodies were used for western blotting: anti-AMPKα (#2603; dilution 1:1000), anti-AMPKα-pT172 (#2535; dilution 1:1000), anti-Raptor (#2280; dilution 1:1000), anti-Raptor-pS792 (#2083; dilution 1:1000), anti-ACC (#3662 (primary cells) #3676 (3T3-L1); dilution 1:1000), anti-ACC-pS79 (#3661; dilution 1:1000), anti-AS160 (#2670 (3T3-L1); dilution 1:1000) anti-AS160-pS588 (#8730; dilution 1:1000), anti-Akt (#9272 (primary cells), #2920 (3T3-L1); dilution 1:1000), anti-Akt-pS473 (#4060 (3T3-L1), 1:2000), anti-Akt-pT308 (#9275; dilution 1:2000), and anti-GSK3α/β

pS21/9 (#9331, dilution 1:1000) were all purchased from Cell Signaling Technology (Danvers, USA). Anti-AMPKβ1-pS108 (#156890, dilution 1:250) was from Abcam, anti-AS160 for primary cells from Merck (#07-741; Darmstadt, Germany; dilution 1:1000). Anti-Akt-pS473 (#44-621G (primary cells), dilution 1:5000), anti-AS160-pT642 (#44-1071G (primary cells), dilution 1:1000) and anti-GSK3α/β (#44-610, dilution 1:2000) were from Thermo Fisher Scientific (Rockford, IL, USA). Anti-β-actin was from Sigma Aldrich. Sheep antibodies used for analysis in 3T3-L1 cells that selectively recognize AS160 phospho-S341, T642 and S751 have been described elsewhere (24) and were kindly provided by Profs. C. Mackintosh and D. G. Hardie (University of Dundee, Dundee, UK). Anti-rabbit and anti-mouse secondary antibodies conjugated to horseradish peroxidase (HRP) were from Thermo Fisher Scientific and GE Healthcare (Uppsala, Sweden) respectively. Donkey infrared dye-labelled anti-mouse and anti-rabbit IgG secondary antibodies were from LI-Cor Biosciences (Cambridge, UK).

Isolation, stimulation and lysis of primary adipocytes.

Mouse adipocytes were isolated by a method similar to that described by Larsson et al. (26) from epididymal adipose tissue of 10-12-wk-old male C57BL/6J BomTac mice (Taconic Biosciences, Ejby, Denmark) or C57BL/6NTac AMPKβ1 S108A knock-in mice, in which the codon in exon 2 encoding S108 was modified to encode alanine (generated by Taconic Biosciences). Rat adipocytes were isolated from 36- to 38-day-old Sprague-Dawley rats (Taconic Biosciences), as described by Berggreen et al. (27). All animals were maintained in the animal facility at the Biomedical Centre, Lund University, Sweden and were housed in conventional shoebox cages with wood chip bedding, 2-4 (rats) or 4-6 (mice) animals per cage in a humidity controlled room with 12-h light/dark cycle and non-restricted access to food and water. Mice and rats were

euthanized at the local animal facility via cervical dislocation or CO_2-sedation followed by decapitation, respectively prior to dissection of epididymal adipose tissue which was then taken to the laboratory for further processing. Animal experiments were approved by the Regional Ethical Committee on Animal Experiments in Malmö/Lund (approval number M286-10 and 5.8.18-18569/2018). Human adipocytes were isolated from abdominal subcutaneous tissue collected from female subjects who underwent reconstructive breast surgery (n=11 individuals, body mass index (BMI) 24.8±3.4 kg/m^2 [mean±SD]). All subjects gave their written informed consent and the studies were approved by the Regional Ethical Review Board at Lund University (approval numbers 2013/298 and 2017/920). Adipocytes were isolated by collagenase (1 mg/ml) digestion in a shaking incubator at 37°C (28). Digests were filtered and washed with Krebs-Ringer medium (120 mM NaCl, 4.7 mM KCl, 1.2 mM KH_2PO_4, 1.2 mM $MgSO_4$) containing 25 mM HEPES pH 7.4, 200 nM adenosine, 2 mM glucose and 1% (w/v) BSA (KRH buffer). After isolation, human adipocytes were incubated overnight in DMEM containing 0.1 mg/ml gentamicin, 3.5% (w/v) BSA and 200 nM PIA at 37°C under 5% CO_2. Subsequently, adipocytes were washed and resuspended in KRH buffer and treated as indicated in the figures. Primary rat and mouse adipocytes were stimulated directly after isolation. In each experiment, cells for the different stimulations were taken from the same cell suspension [1 ml of 8-10% (v/v) cells per stimulation]. Stimulations were performed in singlicate. After stimulation, cells were washed in KRH buffer without BSA and lysed in 50 mM Tris-HCl pH 7.5, 1 mM EGTA, 1 mM EDTA, 1 mM sodium orthovanadate, 10 mM sodium-β-glycerophosphate, 50 mM NaF, 5 mM $Na_4P_2O_7$, 0.27 M sucrose, 1 mM DTT, 1% (w/v) NP40 and complete protease inhibitor (1 tablet/50 ml) (lysis buffer). Lysates were centrifuged at 13 000 g for 15 min at 4°C

and protein concentration in the supernatant was determined according to Bradford using BSA as standard (29).

Culture, stimulation and lysis of 3T3-L1 adipocytes.

3T3-L1 fibroblasts were originally obtained from ATCC and are confirmed to be mycoplasma negative. The cells were cultured and differentiated into adipocytes as described previously (30) and used between passages 7 and 12. Experiments were performed at days 8–12 post differentiation. Stimulation and lysis were performed as described in (20).

Immunoprecipitation of AS160

3T3-L1 adipocyte lysate (200 µg) was added to 0.6 µg of rabbit anti-AS160 antibodies and mixed by rotation overnight at 4°C. Protein A-Sepharose (40 µl of 25% (v/v) slurry in 50 mM Tris-HCl, pH 7.4 at 4°C, 150 mM NaCl, 50 mM NaF, 5 mM $Na_4P_2O_7$, 1 mM EDTA, 1 mM EGTA, 1% (v/v) Triton X-100, 1% (v/v) glycerol, 1 mM dithiothreitol (DTT), 0.1 mM benzamidine, 0.1 mM phenylmethylsulfonyl fluoride, 5 µg/ml soybean trypsin inhibitor and 1 mM Na_3VO_4 (IP buffer)) was added to each sample and mixed by rotation for 3 h at 4°C. The immunoprecipitates were washed three times with 1 ml of IP buffer prior to resuspension in 50 mM Tris-HCl, pH 6.8, 2% (w/v) SDS, 10% (v/v) glycerol, 0.1% (w/v) bromophenol blue and 200 mM DTT (Laemmli sample buffer (LSB)).

Western blotting.

Cell lysates were heated in lithium dodecyl sulfate sample buffer to which DTT (75 mM final concentration) had been added, subjected to electrophoresis on pre-cast Novex 4-12% Bis-Tris gels and subsequently electrotransferred to nitrocellulose membranes.

Membranes were blocked for 30-60 minutes in 50 mM Tris-HCl pH 7.6, 137 mM NaCl and 0.1% (w/v) Tween 20 (TBS-T) containing 10% (w/v) skimmed milk and then probed with primary antibodies in TBS-T containing 5% (w/v) BSA for 16 h at 4°C. Protein detection was performed with HRP-conjugated secondary antibodies and ECL substrate (primary cells) or LI-COR IRdye-conjugated secondary antibodies and a LI-COR Odyssey SA infrared imaging system (3T3-L1 cells) (LI-COR Biosciences Ltd, Cambridge, UK). ECL signals were visualized using a ChemiDoc XRS+ system followed by analysis of band intensities with the software Image Lab 6.0 (both from BioRad; Hercules, CA, USA). LI-COR signals were analysed and quantified using Empiria Software (LI-COR). From the quantified signals, the phospho:total protein ratio was determined and presented - as indicated on the y-axis. To account for variations in absolute values in between experiments, which were run on separate gels and occasions, the data was normalized to a control sample (100 %).

Measurement of glucose uptake in adipocytes.

For primary cells, freshly isolated rodent adipocytes or overnight cultured human adipocytes were washed in glucose free buffer containing 30 mM HEPES pH 7.4, 120 mM NaCl, 4 mM KH_2PO_4, 1 mM $MgSO_4$, 0.75 mM $CaCl_2$, 10 mM $NaHCO_3$, 200 nM adenosine and 1 % (w/v) BSA (incubation buffer). Adipocyte suspensions [400 µl of 2.5 % (v/v) for rat and human cells, or 3.75 and 5 % (v/v) for mouse cells] were pre-incubated with AMPK activators for 1 h before being stimulated with insulin or cytochalasin B (10 µM) for 30 min. Subsequently, 100 µl incubation buffer containing 0.25 µl (0.05µCi) ^{14}C-glucose was added and cells were incubated for a further 30 min. Reactions were stopped by aliquoting 300 µl of each reaction to a Beckman microtube containing 75 µl dinonylphtalate. Microtubes were centrifuged for 1 min at 6000 x g

and frozen at -20°C before the adipocytes were collected and subjected to liquid scintillation counting. All treatments were performed in triplicate.

In 3T3-L1 adipocytes, glucose uptake was measured by the uptake of 2-[^{3}H]-deoxy-D-glucose as described previously (20). Briefly, cells in 128 mM NaCl, 4.7 mM KCl, 5 mM NaH_2PO_4 (pH 7.4), 1.2 mM $MgSO_4$, 2.5 mM $CaCl_2$, 1% (w/v) BSA and 3 mM glucose (Krebs-Ringer-phosphate (KRP) buffer) were stimulated as described, and transport was initiated by adding [^{3}H]-2deoxy glucose (50 µM, 1 µCi/ml). Cells were incubated for 3 min, after which cells were rapidly washed three times in ice-cold PBS, air-dried, and then solubilized in 1% (v/v) Triton X-100. The radioactivity associated with the cells was determined by liquid scintillation counting. Non-specific, cell-associated radioactivity was determined in parallel incubations performed in the presence of 10 µM cytochalasin B.

In order to avoid variations in absolute glucose uptake levels from masking effects of treatments, or potential differences between genotypes, glucose uptake data is presented as percent of a control sample (100 %). To illustrate the variation of absolute values, basal and insulin-stimulated glucose uptake in adipocytes from different species is also presented as absolute values (CPM for rodent and human adipocytes, pmol/min/well for 3T3-L1 adipocytes; Supplementary Figure 1 + 3).

GST-14-3-3 pull-down.

GST-14-3-3 proteins were expressed at 22°C in BL21 (DE3) cells and lysates prepared using a Microfluidizer M-110P cell disrupter set to 20,000 psi in PBS containing 1 mM DTT and protease inhibitor cocktail. Bacterial cell lysates were centrifuged and the supernatant was purified on glutathione-Sepharose beads in 50 mM Tris-HCl pH 8.0. 3T3-L1 adipocyte lysates (100 µg) were pre-cleared with glutathione-Sepharose for 30 min, after which lysates were transferred to fresh tubes containing gluathione-

Sepharose and 50 µg of GST-14-3-3 or GST control. After incubation for 2 h, beads were washed with IP buffer and eluted in LSB containing DTT. AS160 associated with GST-14-3-3 was analyzed by western blotting.

Statistical analysis.

Results are presented as mean with SD of several (number specified in figure legends) independent experiments. Statistical analysis, as indicated in the figure legends, was performed using GraphPad Prism 8 and R-studio. Comparisons to a normalized control (100 %) were performed with a one-sample t-test followed by Bonferroni-Holm correction for multiple comparison, where necessary. For comparisons not involving a normalized control, one- or two-way ANOVA or paired Student's t-test were used.

Results

Differential effect of AMPK activators on glucose uptake in adipocytes.

In order to investigate the effect of AMPK activation on glucose uptake in different adipocyte models, primary rat or human adipocytes or cultured 3T3-L1 cells were pre-incubated with either of the three AMPK activators AICAR, A-769662 or 991, prior to incubation without (basal) or with insulin. As shown in Fig. 1, AICAR treatment significantly inhibited basal as well as insulin-stimulated glucose uptake in primary rat adipocytes (Fig. 1A). Furthermore, pre-incubation with increasing concentrations of A-769662 caused a concentration-dependent inhibition of basal as well as insulin-stimulated glucose uptake (Fig. 1A), to an extent similar to that of AICAR (at the highest concentration of A-769662, 300 µM). However, when rat adipocytes were pre-incubated with 991, no reduction in glucose uptake was observed (Fig. 1A). To ensure that all three activators indeed increased AMPK activity and thus that the observed differential effects were not due to inefficient AMPK activation by 991, AMPK activity status was examined by monitoring the phosphorylation of the AMPK substrates ACC at S79 and Raptor at S792. Fig. 1B shows that all activators induced ACC and Raptor phosphorylation. Furthermore, 30µM 991 induced an even stronger phosphorylation of AMPK substrates than 300 µM A-769662 (Fig. 1B), which was expected as 991 is more potent and binds AMPK 5-10-fold tighter than A-769662 in cell-free assays (12). These results are in line with our previous study showing efficient activation of AMPK by A-769662 and 991 in adipocytes from different primary adipocyte models (18). In addition to rat adipocytes, the effect of AMPK activation on glucose uptake was also investigated in human adipocytes isolated from subcutaneous adipose tissue. Similar to rat adipocytes, A-769662 inhibited basal and insulin-stimulated glucose uptake in a concentration-dependent manner (Fig. 1C) whereas again, no reduction was observed

with 991 (Fig. 1D). In agreement with observations in primary cells, pre-incubation with AICAR (Fig. 1E) or A-769662 (Fig. 1F) significantly reduced insulin-stimulated glucose uptake in 3T3-L1 adipocytes. Whereas A-769662 also significantly reduced basal glucose uptake (Fig. 1F), AICAR was without an effect in untreated cells (Fig. 1E). As in primary cells, pre-incubation with 991 had no effect on basal or insulin-stimulated glucose uptake (Fig. 1G) in 3T3-L1 cells. As shown by increased ACC S79 phosphorylation in Fig 3 A-C, all three activators induced efficient AMPK activation in 3T3-L1 cells. The absolute level of glucose uptake (Supplementary Fig. 1) varied in between experiments, especially in humans (Supplementary Fig. 1B+C) but was significantly induced by insulin in all three adipocyte models (Supplementary Fig. 1).

Differential effects of AMPK activators on glucose uptake cannot be explained by altered insulin signaling.

To explore potential reasons for the differential effects of A-769662 and 991 on glucose uptake, we examined if AMPK activation induces changes in the insulin signaling pathway in primary adipocytes, with a focus on the activation of Akt. Incubation with A-769662 (300 µM) or 991 for 1 h had no significant effect on insulin-stimulated Akt S473 (Fig. 2A) or T308 (Fig. 2B) phosphorylation, in rat adipocytes. However, when pre-treating with AICAR, a significant decrease in Akt S473 phosphorylation was observed (Fig. 2A). When monitoring the effect of AMPK activation on phosphorylation of the Akt substrates GSK3α/β at S21/S9 (Fig. 2C) and AS160 at T642 (Fig. 2D), a significant increase in basal GSK3α/β S21/S9 phosphorylation was detected with AICAR (Fig. 2C), whereas A-769662 (300 µM) and 991 induced no significant changes. To exclude the possibility that A-769662 induces changes in insulin signaling at an earlier time point, the effect of A-769662 was measured at different time points within the first 30 min of insulin stimulation (Fig. 2E-G). Compared to the negative control (without

activator), A-769662 did not induce any significant changes in the phosphorylation of Akt (Fig. 2E), GSK3α/β (Fig. 2F) or AS160 (Fig. 2G) at any of the time points.

A-769662 rapidly inhibits glucose uptake in 3T3-L1 adipocytes yet independently of changes in AS160 phosphorylation.

To identify potential mechanisms underlying the reduced glucose uptake observed in response to A-769662, 3T3-L1 adipocytes were used for more detailed studies of insulin signaling, mainly at the level of AS160, and to explore possible direct effects on the glucose uptake machinery. As shown in Fig. 3A-C, basal Akt S473 phosphorylation was significantly increased in response to AICAR (Fig. 3A), whereas A-769662 (Fig. 3B) and 991 (Fig. 3C) had no significant effect. Insulin-stimulated Akt S473 phosphorylation was also significantly increased by AICAR (A), while A-769662 induced a significant reduction (B) and 991 showed no effect (C). As with primary rat adipocytes in Fig. 1B, the stimulation of AMPK activity by all three activators was confirmed by increased ACC S79 phosphorylation (Fig. 3A-C). In addition to T642, which we monitored in rat adipocytes, AS160 has been shown to be phosphorylated at multiple sites that have been proposed to regulate activity and GLUT4 trafficking (24, 25, 31). As shown in Fig. 3A-E, insulin stimulated the phosphorylation of AS160 at the four sites T642 (Fig. 3A-C; quantified in Supplementary Fig. 2A-C), S341 (Fig. 3A-C; quantified in Supplementary Fig. 2D-F), S588 (Fig. 3C+D; effect of 991 quantified in Supplementary Fig. 2G) and S751 (Fig. 3E). Pre-incubation with A-769662, but not AICAR (Fig. 3D) or 991 (Fig. 3C; Supplementary Fig. 2G), tended to increase basal AS160 S588 phosphorylation, however this effect was not statistically significant. Furthermore, insulin-stimulated AS160 S751 phosphorylation was reduced in response to A-769662 and AICAR (Fig. 3E). Phosphorylation of AS160 at T642 and S341 was not significantly changed in response to any of the three AMPK activators

under basal or insulin-stimulated conditions (Fig. 3A-C, Supplementary Fig. 2A-F). To investigate if any of the observed changes in Akt or AS160 phosphorylation influenced the binding of AS160 to 14-3-3, a pulldown assay with GST-tagged 14-3-3 was performed on lysates from 3T3-L1 adipocytes pre-incubated in the presence or absence of AICAR or A-769662 prior to insulin stimulation. As expected, insulin increased the association of AS160 with 14-3-3, but neither AICAR nor A-769662 treatment influenced this association (Fig. 3F). Collectively, the minor effects of A-769662 on insulin signaling, including AS160 phosphorylation, are not likely to explain the inhibition of glucose uptake by this activator. We therefore speculated that A-769662 might inhibit uptake in a more direct manner and tested this idea by taking advantage of the short incubation time of 3 min with [^{3}H]2-deoxyglucose in the glucose uptake assay for 3T3-L1 adipocytes. A-769662 markedly inhibited basal and insulin-stimulated glucose uptake when added only during the final 3 min of the assay, along with the [^{3}H]2-deoxyglucose, and thus 12 min after insulin was added, suggesting a very rapid inhibitory effect of A-769662 (Fig. 3G). Furthermore, in cells incubated with A-769662 for 30 min prior to insulin stimulation, removal of A-769662 prior to the addition of [^{3}H]2-deoxyglucose did not prevent its inhibitory effect on glucose uptake (Fig. 3H). The absolute level of glucose uptake, and its induction by insulin, is shown in Supplementary Fig. 2H+I.

The effect of A-769662 on glucose uptake is independent of AMPK activation.

Our results so far indicate that the inhibitory effect of A-769662 on glucose uptake might be independent of AMPK activation. To address this issue, an AMPK knock-in mouse model with deficient phosphorylation of S108 in the AMPK β-subunit (AMPKβ1 S108A) was employed. The lack of AMPKβ1 S108 phosphorylation in the mutant was confirmed by western blotting of isolated adipocytes treated with AMPK activators (Fig.

4A). In order to ensure that AMPK activation by A-769662 in the AMPKβ1 S108A mutant cells was impaired, compared to the WT, AMPK activity was monitored via analysis of AMPKα T172 (Fig. 4B), ACC S79 (Fig. 4C) and Raptor S792 (Fig. 4D) phosphorylation. Indeed, at 150µM A-769662, AMPKα T172 phosphorylation was reduced in cells derived from S108A mutant mice compared to WT cells (Fig. 4B). The increasing phosphorylation of ACC and Raptor in response to A-769662 in WT cells was significantly reduced or abolished in the S108A mutant cells (Fig. 4C-D). AMPK activation by AICAR was unaltered in the mutant cells compared to the WT. After having confirmed impaired AMPK activation by A-769662 in the S108A mutant, insulin-stimulated glucose uptake was measured, after pre-incubation with or without AICAR or increasing concentrations of A-769662. As shown in Fig. 4E (top panel), AICAR significantly reduced insulin-stimulated glucose uptake in WT and S108A cells. Furthermore, A-769662 caused a comparable, concentration-dependent inhibition of glucose uptake in adipocytes derived from both WT and S108A mutant mice (Fig. 4E, top panel). Glucose uptake was significantly induced by insulin in WT and mutant cells (shown for absolute values in Supplementary Fig. 3), with no differences observed between the genotypes concerning basal- or insulin-stimulated glucose uptake (Fig. 4E, bottom panel).

Discussion

Over the past years, AMPK activators have received increased attention as potential therapies for T2D, mainly due to their beneficial effects in liver and muscle (3, 32). Given the importance of adipose tissue glucose uptake for whole-body insulin sensitivity and glucose tolerance (16), we investigated the effect of the ADaM site AMPK activators A-769662 and 991 on glucose uptake in different adipocyte models, including human cells. A key finding of our study is that 991 does not affect glucose uptake, whereas A-769662 inhibits glucose uptake in a manner which is likely to be independent of AMPK activation. Our interpretation of these findings is that acute AMPK activation plays a minor role, if any, in the regulation of glucose uptake in human adipocytes, and that the previously reported effect of AICAR on glucose uptake might also be AMPK-independent. This is in agreement with a recent study by Choi et al. (33) showing that AICAR exerts its blood glucose lowering effect independently of adipocyte AMPK. Furthermore, Choi et al. suggest that AMPK in adipocytes plays a negligible role in the regulation of whole-body glucose metabolism, as mice lacking AMPK catalytic subunit (α1/α2) in adipocytes exhibit no significant alteration in their glucose or insulin tolerance (33).

Interestingly, although both A-769662 and 991 bind to the same allosteric site and activate AMPK through a similar mechanism, we revealed that, while A-769662 significantly inhibited insulin-stimulated glucose uptake, no effect was detected with 991. This was observed in primary cells from epididymal rodent- and subcutaneous human adipose tissue, as well as in cultured murine 3T3-L1 adipocytes, demonstrating that this effect is neither species nor adipose depot-specific. In the present as well as in our previous study (18) we also confirmed that AMPK is efficiently activated by both compounds in all our models and under the conditions used. It is possible that the

differential effect of 991, compared to AICAR and A-769662, is caused by the varying AMPKβ-subunit preferences of the three activators. While 991 acts on both β1 and β2-containing complexes, but with a preference for β1, and A-769662 activates only β1-containing complexes, AICAR, an AMP-mimic, activates AMPK regardless of the β-subunit isoform (12, 34, 35). However, the different activators showed comparable effects in rat and human adipocytes, although human adipocytes appear to express more equal amounts of β1 and β2 compared to rat adipocytes (18). Furthermore, since the effect of A-769662 on glucose uptake appears to be AMPK-independent (discussed below), different isoform preferences are not likely to explain the different effects of A-769662 and 991.

As glucose uptake in adipocytes is stimulated by insulin in an Akt-dependent manner, we wanted to examine potential alterations in Akt phosphorylation/activity in response to the AMPK activators (36). In primary adipocytes, the results revealed a similar effect of A-769662 and 991 on phosphorylation of Akt and its downstream targets, namely, if anything, a tendency to increased phosphorylation. Therefore, changes in proximal insulin signaling are not a likely reason for the differential effect of A-769662 and 991 on glucose uptake in these cells. With AICAR, a significant decrease in Akt S473 phosphorylation was observed, indicating decreased Akt kinase activity. However, no significant reduction in phosphorylation of the Akt downstream target GSK3α/β S21/9 was detected. Moreover, although AS160 T642, which is important for interaction of AS160 with 14-3-3 scaffold proteins and ultimately for glucose uptake (25), was reduced in several experiments, this did not reach statistical significance. This observation is in slight contrast to a study by Gaidhu et al., who demonstrated no effect on insulin-induced Akt or GSK3 phosphorylation, but significantly reduced AS160 T642 phosphorylation in response to AICAR (22). The insulin concentration used by Gaidhu

et al. was 10-fold higher, which could provide a possible explanation for the more pronounced effect they observed. However, we do not exclude the possibility that AICAR reduces Akt activity towards AS160 in primary adipocytes, and that this could contribute to AICAR-induced inhibition of glucose uptake in these cells. In 3T3L1 cells however, we observed no reduction in Akt or downstream events. Similar to primary cells, insulin-stimulated glucose uptake was inhibited by A-769662 also in 3T3-L1 adipocytes. In these cells, inhibition of glucose uptake was accompanied by decreased Akt S473 phosphorylation, which however did not translate into changes in AS160 phosphorylation at T642 or its interaction with 14-3-3.

It has been shown that AS160 is phosphorylated at several residues, in addition to T642, in response to insulin stimulation, involving different upstream kinases, such as Akt and AMPK (24, 31). In our detailed analysis of the effects of AMPK activation on AS160 phosphorylation in 3T3-L1 adipocytes, we observed tendencies to an increase in basal AS160 S588 phosphorylation in response to A-769662, and a significant decrease in insulin-stimulated pS751 by AICAR and A-769662. While increased AS160 S588 phosphorylation in response to AMPK activation has been reported previously (24), we are, to our knowledge, the first to report decreased AS160 S751 phosphorylation. The functional role of phosphorylation at these two sites has not been revealed, but does not seem to include 14-3-3 binding, which is mainly mediated by phosphorylation on S341 and T642 – both of which remained unchanged in response to activation of AMPK in 3T3L1 cells in our study (25). In line with this, AMPK activation did not induce any changes in the ability of AS160 to bind 14-3-3.

Up to this point, our data showed that alterations in insulin signaling or AS160 phosphorylation provide no explanation for the differential effects of A-769662 and 991 on glucose uptake. This finding led us to hypothesize that the effect of A-769662 on

glucose uptake might be independent of AMPK activation, which would also be in line with A-769662 showing more off target effects than 991 in *in vitro* kinase screens (37, 38). In order to test this idea, a knock-in mouse model expressing non-phosphorylatable AMPKβ1 S108A was employed. Strikingly, although induction of AMPK activity towards downstream targets by A-769662 was almost absent in AMPKβ1 S108A mutant adipocytes, insulin-stimulated glucose uptake was reduced by A-769662 to the same degree as in WT adipocytes. This result clearly demonstrates that increased AMPK activity is not required for A-769662 to inhibit glucose uptake in adipocytes.

Trafficking of GLUT4 vesicles, i.e. their fusion and/or formation, and ultimately transport of glucose, involves a multitude of proteins, all of which could be possible targets for A-769662 (39). When we added A-769662 together with [^{3}H]2-deoxyglucose for 3 min, we noted that this was sufficient to significantly inhibit glucose uptake in 3T3-L1 adipocytes despite the cells having been stimulated with insulin for the previous 12 min. This rapid response, together with the finding that the effect of A-769662 on glucose uptake is AMPK-independent, indicates a direct effect on GLUT4 itself or on GLUT4 translocation. Additionally, our observation that the inhibitory effect of A-769662 persists even when removing the activator before measurement of glucose uptake could suggest a strong interaction. However, further investigations are required to elucidate the exact mechanism behind A-769662-induced inhibition of glucose uptake.

In summary, in this study we showed that the ADaM site-binding AMPK activators A-769662 and 991 have differential effects on glucose uptake in adipocytes. While A-769662 significantly decreased glucose uptake, 991, despite robustly activating AMPK, showed no effect on glucose uptake in rodent or human adipocytes. We also

provide compelling evidence that the effect observed with A-769662 is likely to be AMPK-independent and might involve direct inhibition of GLUT4 transporters or their trafficking. Taken together, these results suggest that activation of adipocyte AMPK does not inhibit glucose uptake into adipocytes, as previously suggested with AICAR. Our study also highlights the fact that activators, although having the same mode of action, may have different off-target effects.

Acknowledgements

The authors thank Maria Lindahl for outstanding technical support. Mark Rider (Brussels, Belgium), Matt Sanders (Lausanne, Switzerland) and Karin Stenkula are acknowledged for valuable discussions. Jens Martin Larsson, Britt-Louise Boman, Maria Borg Jönsson, Henny Svensson, Carolin Freccero and co-workers at the Department of Plastic and Reconstructive Surgery in Malmö (Sweden) are gratefully acknowledged for the delivery of human adipose tissue.

Funding

This work was financially supported by The Swedish Research Council (project grant Dnr 2017-01295, Linnaeus grant Dnr 349-2006-237, and the Strategic Research Area Exodiab Dnr 2009-1039), The Swedish Foundation for Strategic Research Dnr IRC15-0067, the Swedish Diabetes Foundation, the Påhlsson Foundation, Diabetes UK (Alec and Beryl Warren award BDA09/0003904 and equipment grant BDA11/0004309 to IPS) and research scholarships from King Saud University to YA and King Abdulaziz University to FA.

Conflict of interest

The authors declare that there is no duality of interest associated with this manuscript.

Contribution statement

Conception and design of experiments: FK, YA, SB, ED, KS, IPS, OG.

Performed experiments: FK, YA, SB, FA.

Analysis and interpretation of the data: FK, YA, SB, FA, ED, KS, IPS, OG.

Drafted the manuscript: FK

Edited and revised the manuscript: YA, SB, FA, ED, KS, IPS, OG.

Final version of the manuscript was approved by: FK, YA, SB, FA, ED, IPS, KS, OG

References

1. Carling D. AMPK signalling in health and disease. Curr Opin Cell Biol. 2017;45:31-7.
2. Herzig S, Shaw RJ. AMPK: guardian of metabolism and mitochondrial homeostasis. Nature reviews Molecular cell biology. 2018;19(2):121-35.
3. Steinberg GR, Carling D. AMP-activated protein kinase: the current landscape for drug development. Nat Rev Drug Discov. 2019;18(7):527-51.
4. Corton JM, Gillespie JG, Hawley SA, Hardie DG. 5-aminoimidazole-4-carboxamide ribonucleoside. A specific method for activating AMP-activated protein kinase in intact cells? European journal of biochemistry. 1995;229(2):558-65.
5. Sullivan JE, Brocklehurst KJ, Marley AE, Carey F, Carling D, Beri RK. Inhibition of lipolysis and lipogenesis in isolated rat adipocytes with AICAR, a cell-permeable activator of AMP-activated protein kinase. FEBS letters. 1994;353(1):33-6.
6. Sullivan JE, Carey F, Carling D, Beri RK. Characterisation of 5'-AMP-activated protein kinase in human liver using specific peptide substrates and the effects of 5'-AMP analogues on enzyme activity. Biochem Biophys Res Commun. 1994;200(3):1551-6.
7. Foretz M, Hebrard S, Leclerc J, Zarrinpashneh E, Soty M, Mithieux G, et al. Metformin inhibits hepatic gluconeogenesis in mice independently of the LKB1/AMPK pathway via a decrease in hepatic energy state. The Journal of clinical investigation. 2010;120(7):2355-69.
8. Guigas B, Bertrand L, Taleux N, Foretz M, Wiernsperger N, Vertommen D, et al. 5-Aminoimidazole-4-carboxamide-1-beta-D-ribofuranoside and metformin inhibit hepatic glucose phosphorylation by an AMP-activated protein kinase-independent effect on glucokinase translocation. Diabetes. 2006;55(4):865-74.
9. Mottillo EP, Desjardins EM, Crane JD, Smith BK, Green AE, Ducommun S, et al. Lack of Adipocyte AMPK Exacerbates Insulin Resistance and Hepatic Steatosis through Brown and Beige Adipose Tissue Function. Cell metabolism. 2016;24(1):118-29.
10. Collodet C, Foretz M, Deak M, Bultot L, Metairon S, Viollet B, et al. AMPK promotes induction of the tumor suppressor FLCN through activation of TFEB independently of mTOR. FASEB journal : official publication of the Federation of American Societies for Experimental Biology. 2019;33(11):12374-91.

11. Cool B, Zinker B, Chiou W, Kifle L, Cao N, Perham M, et al. Identification and characterization of a small molecule AMPK activator that treats key components of type 2 diabetes and the metabolic syndrome. Cell metabolism. 2006;3(6):403-16.
12. Xiao B, Sanders MJ, Carmena D, Bright NJ, Haire LF, Underwood E, et al. Structural basis of AMPK regulation by small molecule activators. Nature communications. 2013;4:3017.
13. Sanders MJ, Ali ZS, Hegarty BD, Heath R, Snowden MA, Carling D. Defining the mechanism of activation of AMP-activated protein kinase by the small molecule A-769662, a member of the thienopyridone family. The Journal of biological chemistry. 2007;282(45):32539-48.
14. Jorgensen SB, Richter EA, Wojtaszewski JF. Role of AMPK in skeletal muscle metabolic regulation and adaptation in relation to exercise. The Journal of physiology. 2006;574(Pt 1):17-31.
15. Viollet B, Foretz M, Guigas B, Horman S, Dentin R, Bertrand L, et al. Activation of AMP-activated protein kinase in the liver: a new strategy for the management of metabolic hepatic disorders. The Journal of physiology. 2006;574(Pt 1):41-53.
16. Abel ED, Peroni O, Kim JK, Kim YB, Boss O, Hadro E, et al. Adipose-selective targeting of the GLUT4 gene impairs insulin action in muscle and liver. Nature. 2001;409(6821):729-33.
17. Smith U, Kahn BB. Adipose tissue regulates insulin sensitivity: role of adipogenesis, de novo lipogenesis and novel lipids. Journal of internal medicine. 2016;280(5):465-75.
18. Kopietz F, Berggreen C, Larsson S, Sall J, Ekelund M, Sakamoto K, et al. AMPK activation by A-769662 and 991 does not affect catecholamine-induced lipolysis in human adipocytes. Am J Physiol Endocrinol Metab. 2018.
19. Gaidhu MP, Fediuc S, Ceddia RB. 5-Aminoimidazole-4-carboxamide-1-beta-D-ribofuranoside-induced AMP-activated protein kinase phosphorylation inhibits basal and insulin-stimulated glucose uptake, lipid synthesis, and fatty acid oxidation in isolated rat adipocytes. The Journal of biological chemistry. 2006;281(36):25956-64.
20. Salt IP, Connell JM, Gould GW. 5-aminoimidazole-4-carboxamide ribonucleoside (AICAR) inhibits insulin-stimulated glucose transport in 3T3-L1 adipocytes. Diabetes. 2000;49(10):1649-56.
21. Yamaguchi S, Katahira H, Ozawa S, Nakamichi Y, Tanaka T, Shimoyama T, et al. Activators of AMP-activated protein kinase enhance GLUT4 translocation and its

565 glucose transport activity in 3T3-L1 adipocytes. Am J Physiol Endocrinol Metab.
566 2005;289(4):E643-9.
567 22. Gaidhu MP, Perry RL, Noor F, Ceddia RB. Disruption of AMPKalpha1 signaling
568 prevents AICAR-induced inhibition of AS160/TBC1D4 phosphorylation and glucose
569 uptake in primary rat adipocytes. Mol Endocrinol. 2010;24(7):1434-40.
570 23. Sano H, Kane S, Sano E, Miinea CP, Asara JM, Lane WS, et al. Insulin-
571 stimulated phosphorylation of a Rab GTPase-activating protein regulates GLUT4
572 translocation. The Journal of biological chemistry. 2003;278(17):14599-602.
573 24. Geraghty KM, Chen S, Harthill JE, Ibrahim AF, Toth R, Morrice NA, et al.
574 Regulation of multisite phosphorylation and 14-3-3 binding of AS160 in response to
575 IGF-1, EGF, PMA and AICAR. The Biochemical journal. 2007;407(2):231-41.
576 25. Ramm G, Larance M, Guilhaus M, James DE. A role for 14-3-3 in insulin-
577 stimulated GLUT4 translocation through its interaction with the RabGAP AS160. The
578 Journal of biological chemistry. 2006;281(39):29174-80.
579 26. Larsson S, Jones HA, Goransson O, Degerman E, Holm C. Parathyroid
580 hormone induces adipocyte lipolysis via PKA-mediated phosphorylation of hormone-
581 sensitive lipase. Cellular signalling. 2016;28(3):204-13.
582 27. Berggreen C, Gormand A, Omar B, Degerman E, Goransson O. Protein kinase
583 B activity is required for the effects of insulin on lipid metabolism in adipocytes. Am J
584 Physiol Endocrinol Metab. 2009;296(4):E635-46.
585 28. Henriksson E, Sall J, Gormand A, Wasserstrom S, Morrice NA, Fritzen AM, et
586 al. SIK2 regulates CRTCs, HDAC4 and glucose uptake in adipocytes. J Cell Sci.
587 2015;128(3):472-86.
588 29. Bradford MM. A rapid and sensitive method for the quantitation of microgram
589 quantities of protein utilizing the principle of protein-dye binding. Analytical
590 biochemistry. 1976;72:248-54.
591 30. Katwan OJ, Alghamdi F, Almabrouk TA, Mancini SJ, Kennedy S, Oakhill JS, et
592 al. AMP-activated protein kinase complexes containing the beta2 regulatory subunit
593 are up-regulated during and contribute to adipogenesis. The Biochemical journal.
594 2019;476(12):1725-40.
595 31. Chen S, Murphy J, Toth R, Campbell DG, Morrice NA, Mackintosh C.
596 Complementary regulation of TBC1D1 and AS160 by growth factors, insulin and AMPK
597 activators. The Biochemical journal. 2008;409(2):449-59.

32. Hardie DG. AMPK: A Target for Drugs and Natural Products With Effects on Both Diabetes and Cancer. Diabetes. 2013;62(7):2164-72.
33. Choi RH, McConahay A, Johnson MB, Jeong HW, Koh HJ. Adipose tissue-specific knockout of AMPKalpha1/alpha2 results in normal AICAR tolerance and glucose metabolism. Biochem Biophys Res Commun. 2019;519(3):633-8.
34. Lai YC, Kviklyte S, Vertommen D, Lantier L, Foretz M, Viollet B, et al. A small-molecule benzimidazole derivative that potently activates AMPK to increase glucose transport in skeletal muscle: comparison with effects of contraction and other AMPK activators. The Biochemical journal. 2014;460(3):363-75.
35. Rajamohan F, Reyes AR, Frisbie RK, Hoth LR, Sahasrabudhe P, Magyar R, et al. Probing the enzyme kinetics, allosteric modulation and activation of alpha1- and alpha2-subunit-containing AMP-activated protein kinase (AMPK) heterotrimeric complexes by pharmacological and physiological activators. The Biochemical journal. 2016;473(5):581-92.
36. Bogan JS. Regulation of glucose transporter translocation in health and diabetes. Annu Rev Biochem. 2012;81:507-32.
37. Bultot L, Jensen TE, Lai YC, Madsen AL, Collodet C, Kviklyte S, et al. Benzimidazole derivative small-molecule 991 enhances AMPK activity and glucose uptake induced by AICAR or contraction in skeletal muscle. Am J Physiol Endocrinol Metab. 2016;311(4):E706-e19.
38. Goransson O, McBride A, Hawley SA, Ross FA, Shpiro N, Foretz M, et al. Mechanism of action of A-769662, a valuable tool for activation of AMP-activated protein kinase. The Journal of biological chemistry. 2007;282(45):32549-60.
39. Wardzala LJ, Cushman SW, Salans LB. Mechanism of insulin action on glucose transport in the isolated rat adipose cell. Enhancement of the number of functional transport systems. The Journal of biological chemistry. 1978;253(22):8002-5.

Figure legends

Figure 1. Differential effects of AMPK activators on glucose uptake in adipocytes.

(A-D) Primary adipocytes isolated from rat epididymal adipose tissue (A+B) or subcutaneous human adipose tissue (C+D) were pre-incubated with 2 mM AICAR (A-D), A-769662 (A-C) or 991 (A+D) for 1 h or left untreated as indicated. Subsequently, cells were stimulated with (white bars) or without (basal; black bars) insulin for a further 30 min before measurement of ^{14}C-glucose uptake. Data is presented as percent of each negative control and graphs show means +SD of 4-7 independent experiments. (B) Phosphorylation of ACC S79 and Raptor S792 was analyzed by western blot with phospho-specific antibodies (n = 4 independent experiments). pACC S79 signals were quantified and expressed as percent of the basal, AICAR-treated sample. (E-G) 3T3-L1 adipocytes were pre-treated with 2 mM AICAR (E), 300 µM A-769662 (F) or 5 µM 991 (G) for 30 min or left untreated before stimulation with (white bars) or without (black bars) 10nM insulin for an additional 15 min as indicated. [^{3}H]-2-deoxyglucose uptake was measured over the final 3 min. Data is presented as percent of the insulin-stimulated negative control and graphs represent means +SD of 6-19 independent experiments. Statistical significance was determined by one-sample t-test followed by Bonferroni-Holm correction for multiple comparison when investigating changes relative an internal control set to 100% (A-F), and one-way ANOVA followed by Holm-Sidak's multiple comparison test (B) or paired Student's t-test followed by Bonferroni-Holm correction for multiple comparison (F), when making comparisons not involving the internal control. *p<0.05, **p<0.01, ***p<0.001, ****p<0.0001, ns=non-significant.

Figure 2. AMPK activation is not associated with impaired insulin signaling in primary adipocytes.

649 Primary rat adipocytes were pre-treated with 2 mM AICAR, 300 µM A-769662, 991 or
650 left untreated as indicated in the figure for 1 h prior to stimulation with (white bars) or
651 without (black bars) 10 nM insulin for 30 min (A-D) or the indicated time periods (E-G).
652 Phosphorylation of Akt S473 (A+E), Akt T308 (B+E), pGSK3α/β S21/9 (C+F) and
653 AS160 T642 (D+G) was analyzed by western blot using phospho-specific antibodies.
654 Signals were quantified and normalized to total protein levels. Data is presented as
655 percent of the insulin-stimulated negative control (A-D) or the 5 min insulin-stimulated
656 negative control (E-G). Graphs represent means +SD (A-D) or ±SD (E-G) of 3-4
657 independent experiments. Representative western blots are shown. Statistical
658 significance was determined by one-sample t-test (A+B) or paired Student's t-test and
659 one sample t-test, followed by Bonferroni-Holm correction for multiple comparison
660 (C+D). *$p<0.05$, **$p<0.01$, ns=non-significant.

661 *Figure 3. A-769662 rapidly inhibits glucose uptake in 3T3-L1 adipocytes yet*
662 *independently of changes in AS160 phosphorylation.*

663 (A-E) 3T3-L1 adipocytes were pre-treated with 2 mM AICAR, 300 µM A-769662 or 5
664 µM 991 for 30 min or left untreated before stimulation with (white bars) or without (black
665 bars) 10 nM insulin for an additional 15 min as indicated. Phosphorylation of Akt S473
666 (A-C), ACC S79 (A-C) and AS160 at the residues T642 (A-C), S341 (A-C), S588 (C+D)
667 and S751 (E) was analyzed by western blot of whole lysates or AS160
668 immunoprecipitates (IP; for pS751), using phospho-specific antibodies. Western blot
669 signals were quantified, normalized to total protein levels and expressed as percent of
670 the insulin-stimulated negative control. Blots shown are representative of 3-8
671 independent experiments. (F) Cell lysates were incubated with GST-14-3-3
672 immobilized on glutathione-Sepharose and proteins associated with the pellets were

673 subjected to western blot with AS160 antibodies. Immunoblot signals were quantified
674 and expressed as percent of the insulin-stimulated negative control. Representative
675 western blots of 5 independent experiments are shown. (G) 3T3-L1 adipocytes were
676 stimulated with (white bars) or without (black bars) 10 nM insulin for 15 min, and [^{3}H]-
677 2-deoxyglucose uptake was measured in the absence or presence of 300 µM
678 A-769662 over the final 3 min. (H) 3T3-L1 adipocytes were pre-treated with 300µM
679 A-769662 for 30 min or left untreated before stimulation with (white bars) or without
680 (black bars) 10nM insulin for an additional 15 min as indicated. For the final 3 min,
681 buffer was exchanged to remove A-769662 but keep insulin, and [^{3}H]-2-deoxyglucose
682 uptake was measured. (G+H) Data is presented as percent of the insulin-stimulated
683 negative control and graphs represent means +SD of 3 independent experiments.
684 Statistical significance was determined by paired-Student's t-test and one-sample t-
685 test, followed by Bonferroni-Holm correction for multiple comparison. *p<0.05,
686 **p<0.01, ***p<0.001, ns=non-significant.

687 *Figure 4. AMPK activation is not required for inhibition of glucose uptake by A-769662.*
688 (A-D) Primary adipocytes isolated from WT (black bars) or AMPKβ1 S108A knock-in
689 (white bars) mice were incubated for 1 h with 2 mM AICAR or A-769662 as indicated.
690 Phosphorylation of AMPK at the residues S108 (β-subunit; A) or T172 (α-subunit; B),
691 ACC S79 (C) and Raptor S792 (D) was analyzed by western blot using phospho-
692 specific antibodies. Immunoblot signals were quantified and normalized to total protein
693 levels where indicated. Data is expressed as percent of untreated cells of each
694 genotype and presented as means + SD. Blots are representative of 4-11 independent
695 experiments. (E) Primary mouse adipocytes were pre-incubated with 2 mM AICAR or
696 A-769662 for 1 h or left untreated, prior to further stimulation with or without 0.1 nM
697 insulin for 30 min and uptake of ^{14}C-glucose was measured. Insulin-induced glucose

698 uptake is presented as percent of each negative control (top panel) from 3-10
699 independent experiments. The average induction of glucose uptake in the WT and
700 AMPKβ1 S108A mutant was 350 and 360 %, respectively (bottom panel). Graphs
701 show means + SD. Statistical significance was determined by one-way ANOVA (A-D)
702 or one sample t-test (E) and paired Student's t test (E, bottom panel), followed by
703 Bonferroni-Holm correction for multiple comparison. *$p<0.05$, **$p<0.01$, ***$p<0.001$,
704 ns=non-significant.

Figure 1

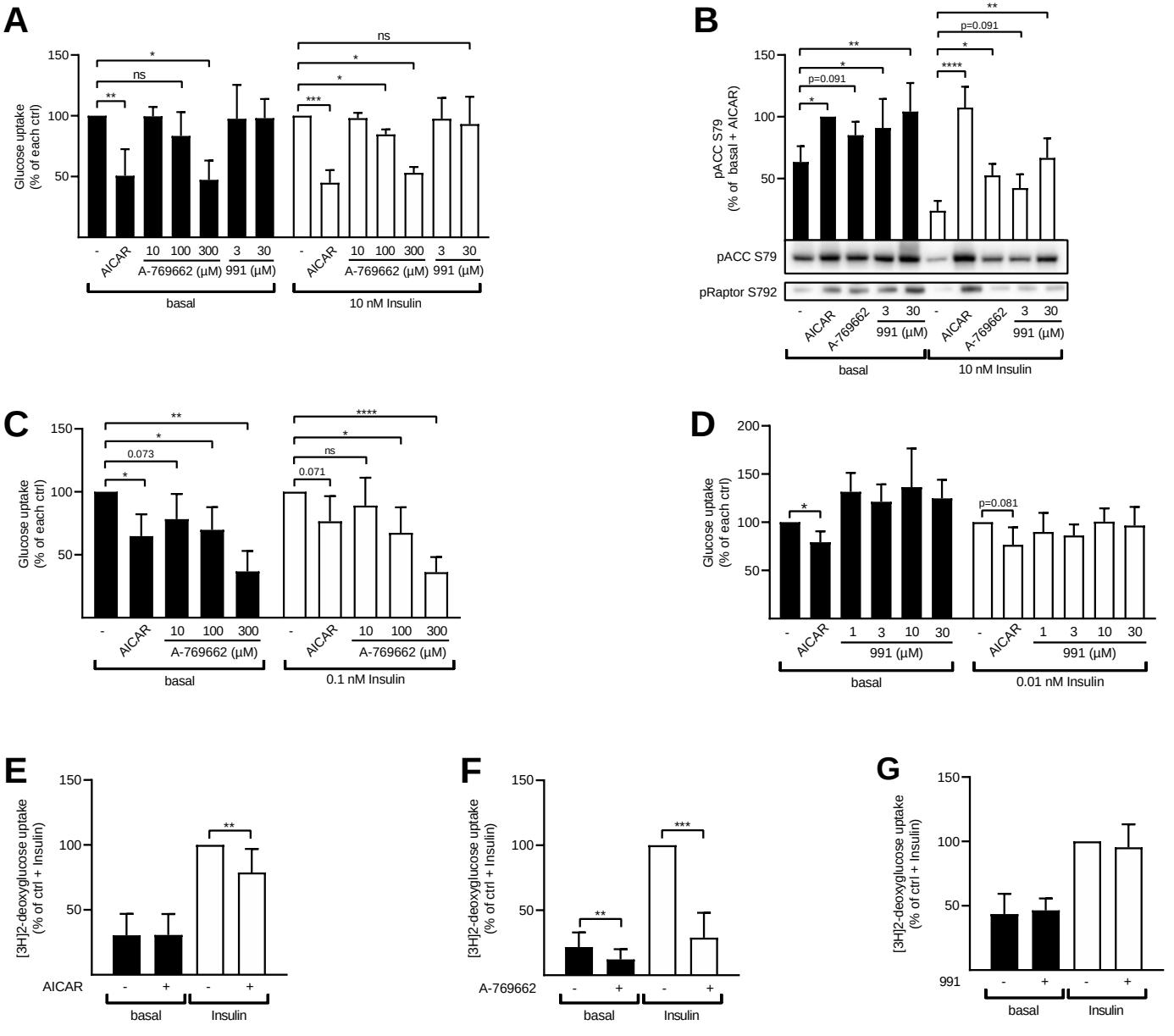
A
Glucose uptake (% of each ctrl)
150
100
50
*
ns
**
***
-
AICAR
10
100
300
3
30
A-769662 (μM)
991 (μM)
basal
10 nM Insulin
B
pACC S79 (% of basal + AICAR)
p=0.091
****
pACC S79
pRaptor S792
A-769662
C
0.073
0.071
0.1 nM Insulin
D
p=0.081
1
0.01 nM Insulin
E
[3H]2-deoxyglucose uptake (% of ctrl + Insulin)
Insulin
F
G
991

Figure 2

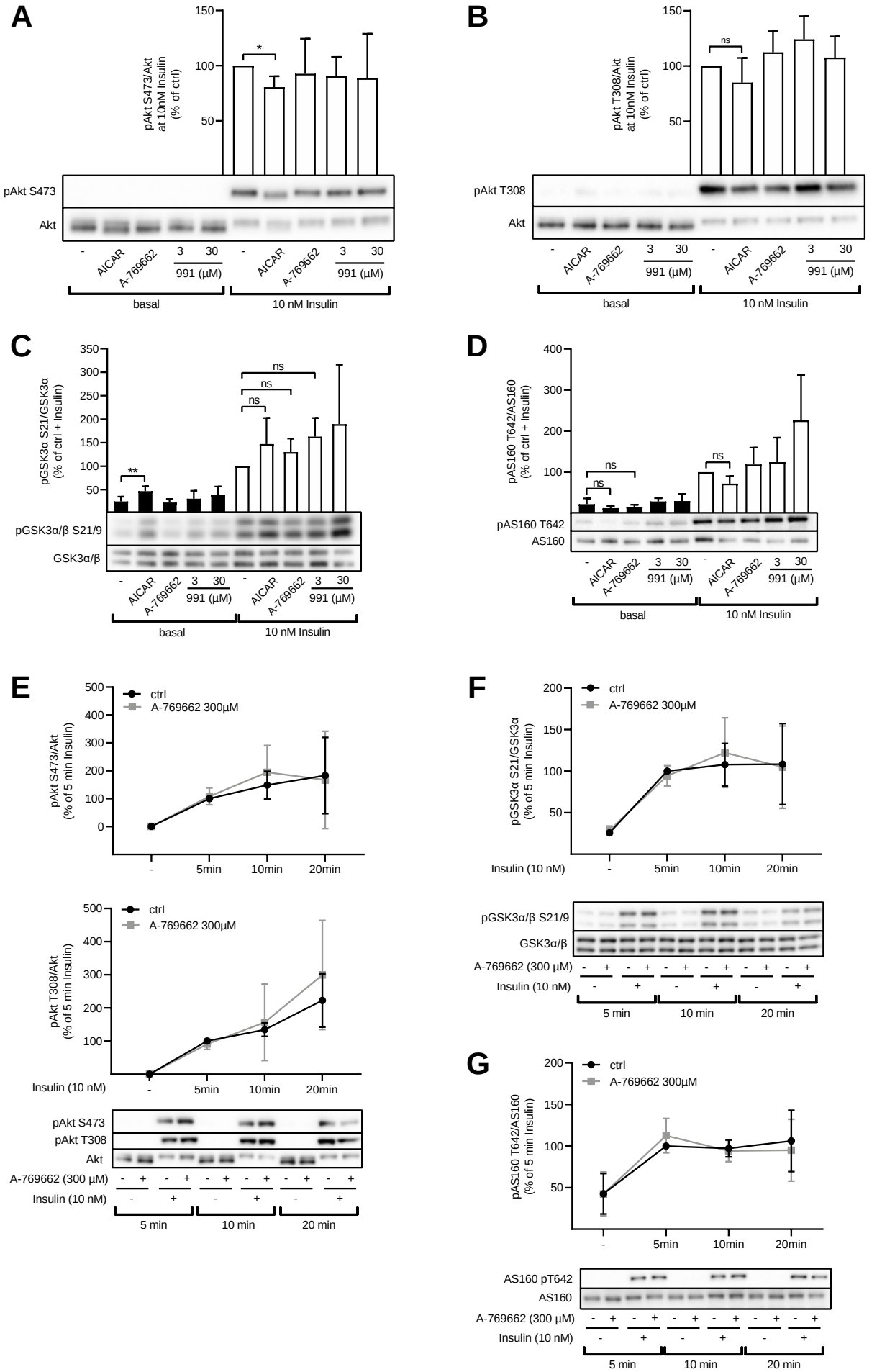
A
pAkt S473/Akt at 10nM Insulin (% of ctrl)
150
100
50
*
pAkt S473
Akt
-
AICAR
A-769662
3
30
991 (μM)
basal
10 nM Insulin
B
pAkt T308/Akt at 10nM Insulin (% of ctrl)
ns
pAkt T308
C
pGSK3α S21/GSK3α (% of ctrl + Insulin)
350
300
250
200
150
100
50
**
ns
pGSK3α/β S21/9
GSK3α/β
D
pAS160 T642/AS160 (% of ctrl + Insulin)
400
pAS160 T642
AS160
E
pAkt S473/Akt (% of 5 min Insulin)
ctrl
A-769662 300μM
500
400
300
200
100
0
5min
10min
20min
pAkt T308/Akt (% of 5 min Insulin)
Insulin (10 nM)
pAkt S473
pAkt T308
Akt
A-769662 (300 μM)
5 min
10 min
20 min
F
pGSK3α S21/GSK3α (% of 5 min Insulin)
pGSK3α/β S21/9
GSK3α/β
G
pAS160 T642/AS160 (% of 5 min Insulin)
AS160 pT642
AS160

Figure 3

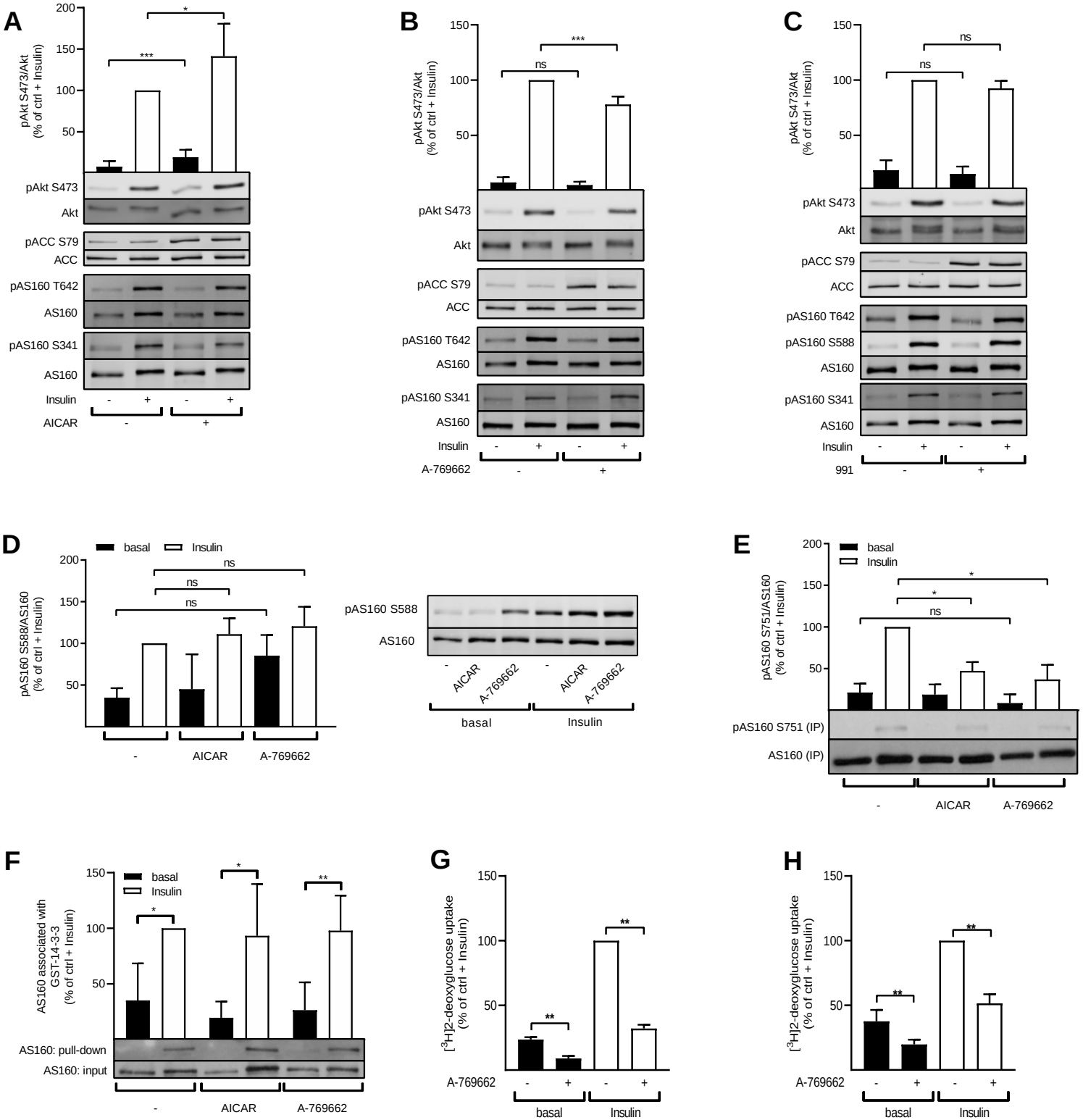
A
pAkt S473/Akt (% of ctrl + Insulin)
pAkt S473
Akt
pACC S79
ACC
pAS160 T642
AS160
pAS160 S341
AS160
Insulin
AICAR
B
pAkt S473/Akt (% of ctrl + Insulin)
pAkt S473
Akt
pACC S79
ACC
pAS160 T642
AS160
pAS160 S341
AS160
Insulin
A-769662
C
pAkt S473/Akt (% of ctrl + Insulin)
pAkt S473
Akt
pACC S79
ACC
pAS160 T642
pAS160 S588
AS160
pAS160 S341
AS160
Insulin
991
D
basal
Insulin
pAS160 S588/AS160 (% of ctrl + Insulin)
AICAR
A-769662
pAS160 S588
AS160
basal
Insulin
E
basal
Insulin
pAS160 S751/AS160 (% of ctrl + Insulin)
pAS160 S751 (IP)
AS160 (IP)
AICAR
A-769662
F
basal
Insulin
AS160 associated with GST-14-3-3 (% of ctrl + Insulin)
AS160: pull-down
AS160: input
AICAR
A-769662
G
[3H]2-deoxyglucose uptake (% of ctrl + Insulin)
A-769662
basal
Insulin
H
[3H]2-deoxyglucose uptake (% of ctrl + Insulin)
A-769662
basal
Insulin

Figure 4

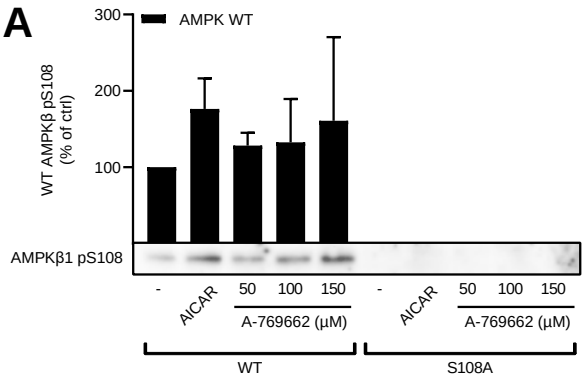
A
AMPK WT
WT AMPKβ pS108 (% of ctrl)
300
200
100
AMPKβ1 pS108
-
AICAR
50
100
150
A-769662 (μM)
WT
S108A

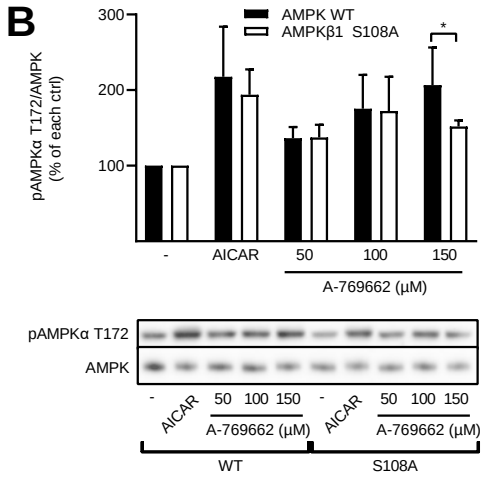
B
AMPK WT
AMPKβ1 S108A
pAMPKα T172/AMPK (% of each ctrl)
300
200
100
*
AICAR
50
100
150
A-769662 (μM)
pAMPKα T172
AMPK
WT
S108A

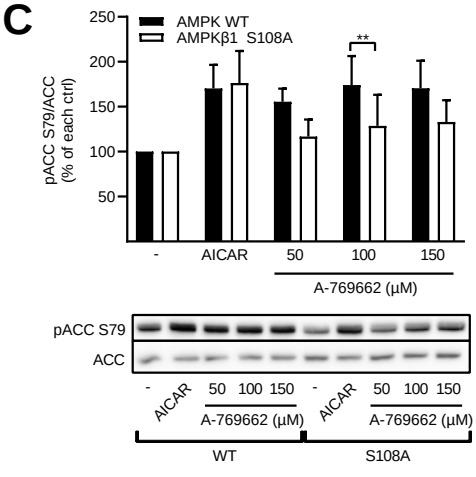
C
AMPK WT
AMPKβ1 S108A
pACC S79/ACC (% of each ctrl)
250
200
150
100
50
**
AICAR
50
100
150
A-769662 (μM)
pACC S79
ACC
WT
S108A

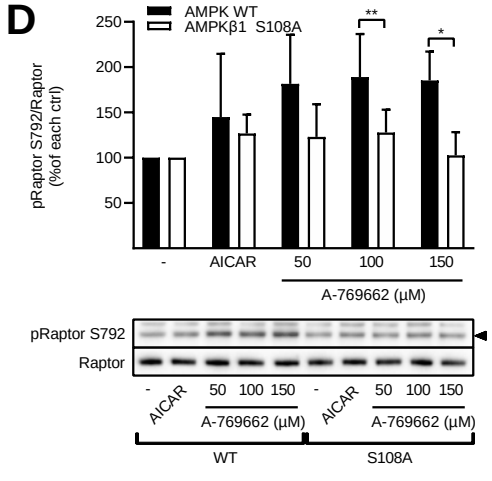
D
AMPK WT
AMPKβ1 S108A
pRaptor S792/Raptor (%of each ctrl)
250
200
150
100
50
**
*
AICAR
50
100
150
A-769662 (μM)
pRaptor S792
Raptor
WT
S108A

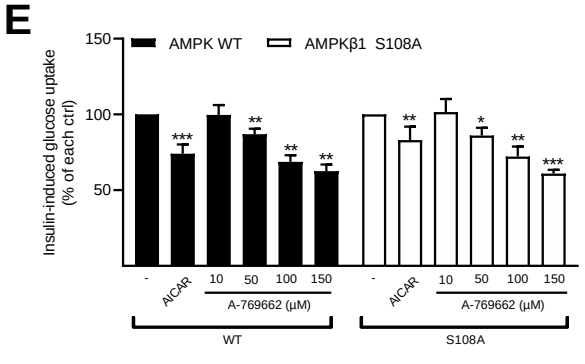
E
AMPK WT
AMPKβ1 S108A
Insulin-induced glucose uptake (% of each ctrl)
150
100
50
***
**
*
AICAR
10
50
100
150
A-769662 (μM)
WT
S108A

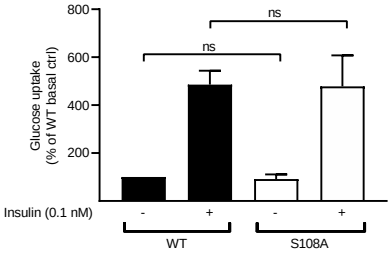
Glucose uptake (% of WT basal ctrl)
800
600
400
200
ns
Insulin (0.1 nM)
-
+
WT
S108A

Figure legends for supplementary data

Supplementary Figure 1. Induction of glucose uptake by insulin as absolute values – connected to Fig. 1. (A, connected to Fig. 1A) Glucose uptake in rat adipocytes shown as absolute values (CPM/30min/10µl PCV). The mean stimulation was 271 %. (B+C, connected to Fig. 1C + D respectively) Glucose Uptake in human adipocytes shown as absolute values (CPM/30min/10µl PCV). The mean stimulation was 63 % (B) and 71 % (C). (D-F, connected to Fig. 1E-F) Glucose uptake in 3T3-L1 adipocytes shown as absolute values (pmol/min/well). The mean stimulation was 445 %. Statistical significance was determined by paired, two-tailed Student's test. *p<0.05, **p<0.01, ***p<0.001, ****p<0.0001,

Supplementary Figure 2. Quantifications of western blots for AS160 pT642, pS341 and pS588 and induction of glucose uptake by insulin in absolute values – connected to Fig. 3. (A-G) Western blot signals for AS160 pT642 (A-C), pS341 (D-F) and pS588 (G) shown in Fig.3 A-C were quantified, normalized to total AS160 protein levels and expressed as percent of the insulin-stimulated negative control. All graphs represent means +SD of 3-8 independent experiments. (H+I) Glucose uptake in 3T3-L1 adipocytes shown as absolute values (pmol/min/well) for Fig. 3 G+H (H connected to Fig. 3G and I to Fig. 3H). Statistical significance was determined by paired Student's t-test (H+I). *p<0.05, ns=non-significant.

Supplementary Figure 3. Induction of glucose uptake by insulin as absolute values – connected to Fig. 4E. Glucose uptake in mouse adipocytes shown as absolute values (CPM/30min/20µl PCV)). The mean stimulation of glucose uptake was 461 % and 494 % in WT and S108A respectively. Statistical significance was determined by 2-way

ANOVA followed by Holm-Sidak's multiple comparison test. ****p<0.0001, ns=non-significant.

Supplementary Figure 1

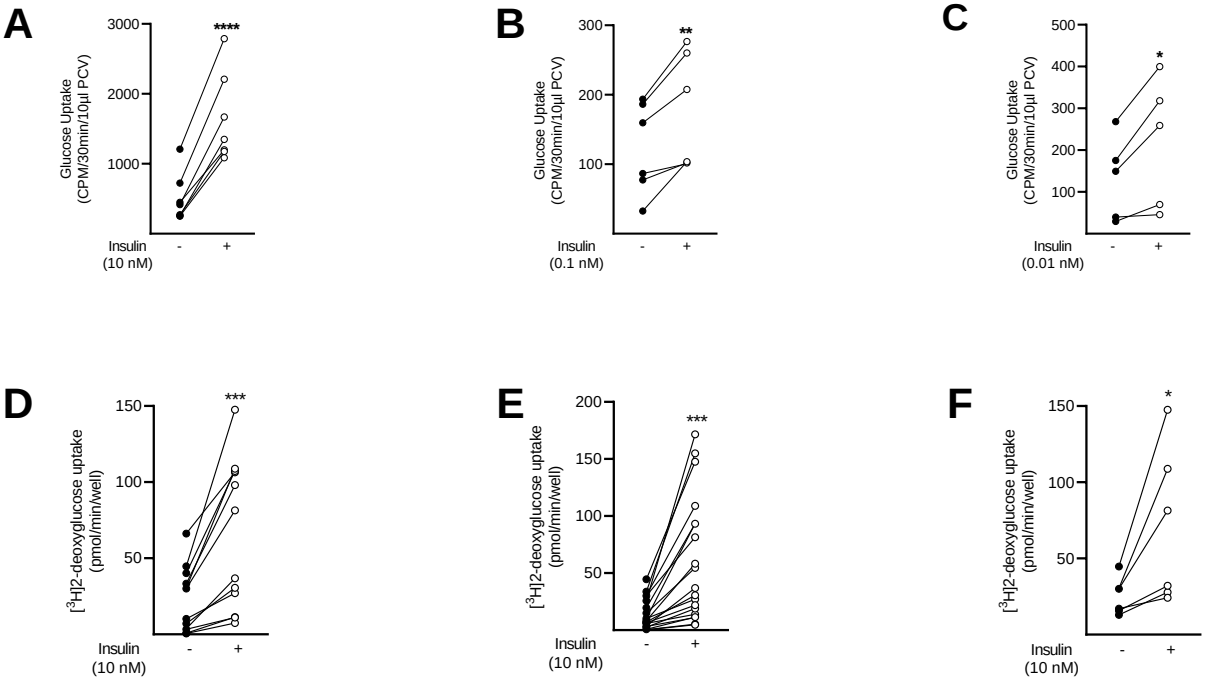

Supplementary Figure 2

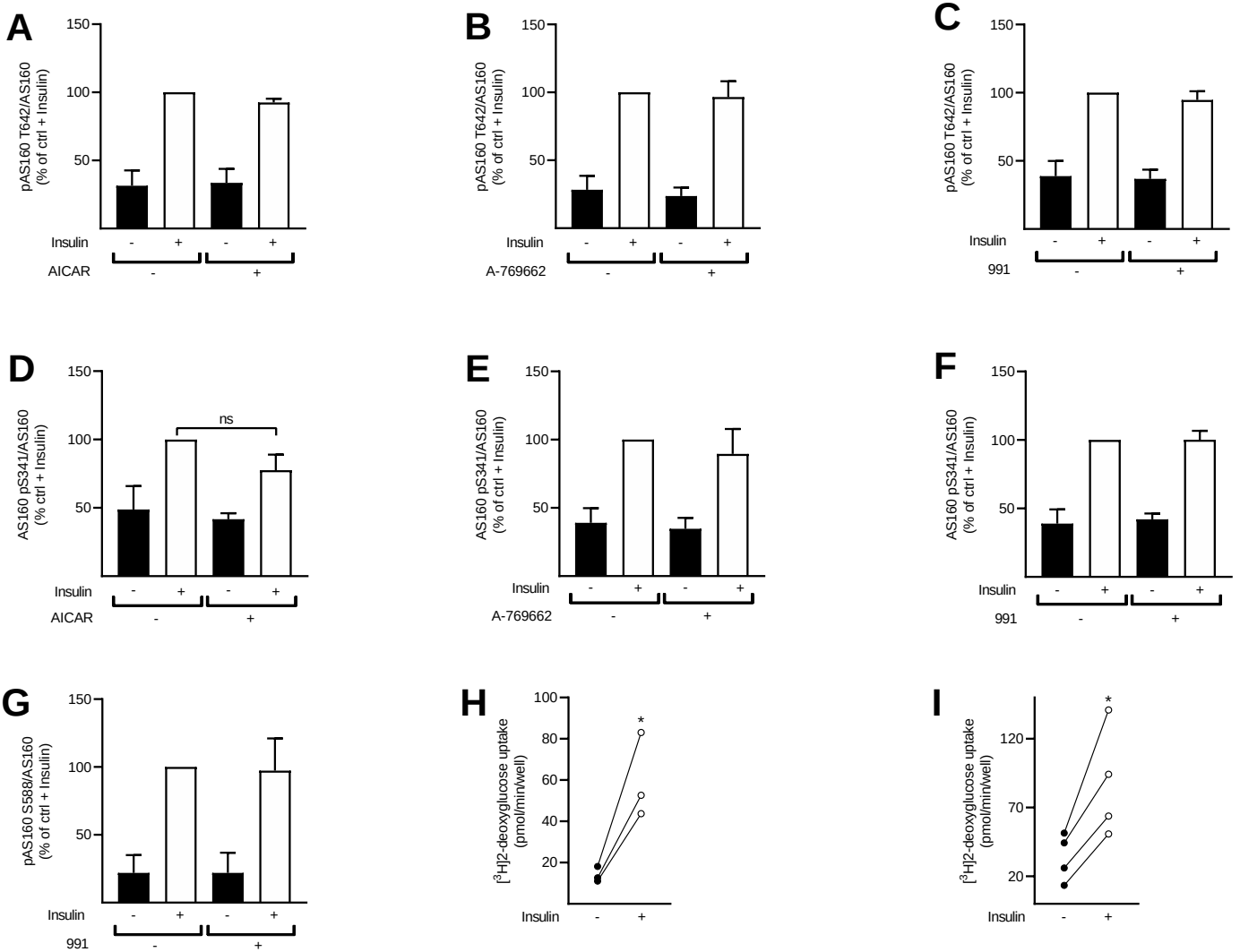

Supplementary Figure 3